MRI SHOULDER COMPLEX SEGMENTATION AND CLASSIFICATION

Gabriela Pérez[1], J. F. Garamendi[2]
[1]*Departamento de Ciencias de la Computación,* [2]*Laboratorio de Imagen Médica y Biometría, Madrid, Spain*

R. Montes Diez[3], E. Schiavi[4]
[3]*Departamento de Estadística e Investigación Operativa,* [4]*Departamento de Matemática Aplicada*

Universidad Rey Juan Carlos, Madrid, Spain

Keywords: MRI, shoulder complex, segmentation, classification, multiphase Chan-Vese model.

Abstract: This paper deals with a segmentation (classification) problem which arises in the diagnostic and treatment of shoulder disorders. Classical techniques can be applied successfully to solve the binary problem but they do not provide a suitable method for the multiphase problem we consider. To this end we compare two different methods which have been applied successfully to other medical images modalities and structures. Our preliminary results suggest that a successful segmentation and classification has to be based on an hybrid method combining statistical and geometric information.

1 INTRODUCTION

Shoulder imaging is one of the major applications in MRI and the primary diagnostic tool in the evaluation of musculoskeletal disease, (Vahlensieck, 2000), (Ehman et al., 2001).

Accurate diagnosis and treatment of painful shoulder and others musculoskeletal complaints and disorders (such as arthritis, abnormalities, bone tumors, worn-out cartilage, torn ligaments, or infection) may prevent from functional loss, instability and disability. Recent interest is also in musculoskeletal tumor and disorders associated with HIV infection and AIDS, (Biviji et al., 2002), (Johnson and Steinbach LS, 2003). In order to provide a reliable method for successful clinical evaluation an increasing effort has to be done in mathematical engineering and biomedical imaging where the specific protocols of 2D segmentation, 3D reconstruction, feature extraction and 4D motion are modeled. In this approach for image guided analysis of shoulder pathologies, automatic and unsupervised segmentation and classification represent the first challenging task. In fact, practical difficulties arise due to the high resolution required for visualization of small but critical structures, to the gross inhomogeneities of field coil response, to the degree of noise present with the signal and to extreme low contrast details between some distinct anatomical structures (fat, bone regions, muscle and tendons, ligaments and cartilage). The existence of a general technique able to cope with all these difficulties for all 3D MRI images sequences is still an open question. A preliminary analysis of the model problem is done here, where a multiphase (2 phases, 4 classes) variational framework is considered for 2D image segmentation and classification. Notice that 2D segmentation is a fundamental step towards the 3D morpho-dynamic reconstruction problem of automatic segmentation. This in turn allows for motion tracking for 4D reconstruction and visualization of musculoskeletal structures.

2 MATERIAL AND METHODS

This contribution is devoted to the preliminary analysis and application of a modified multiphase segmentation and classification algorithm based on previous work of Chan and Vese (Chan and Vese, 2001). This multiphase approach can manage the classification problem underlying the segmentation exercise so broadening the scope of these PDE-based segmenta-

Pérez G., F. Garamendi J., Montes Diez R. and Schiavi E. (2008).
MRI SHOULDER COMPLEX SEGMENTATION AND CLASSIFICATION.
In *Proceedings of the First International Conference on Bio-inspired Systems and Signal Processing*, pages 13-18
DOI: 10.5220/0001067600130018

tion models.

In order to validate our results we compare with a mixture density estimation algorithm for image classification previously presented in (Mignotte et al., 2001), in the context of brain MRI images.
As an application of our method we consider coronal and transverse (axial), 2D MRI shoulder images extracted from two 3D sequences. The images are courtesy of the Ruber International Hospital in Madrid.

The shoulder joint is composed of three bones: the clavicle (collarbone), the scapula (shoulder blade), and the humerus (upper arm bone). The bones of the shoulder are held in place by muscles, tendons and ligaments. Tendons are tough cords of tissue that attach the shoulder muscles to bone and assist the muscles in moving the shoulder. Ligaments attach shoulder bones to each other, providing stability. The ends bones are covered by cartilage which provides painless motion. See Figure 1.

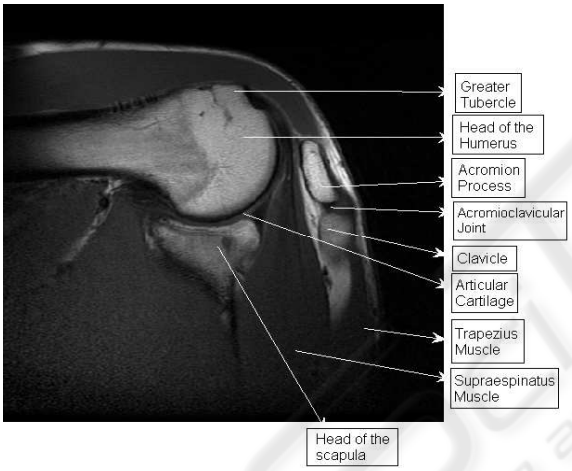

Figure 1: Components of the shoulder, Coronal MR image.

The classification problem we are about can be considered in the framework of minimal partition problems (Mumford-Shah) and cannot be dealt with classical techniques whereas binarization of image sequence is not suitable to produce the segmentation of all the classes we are interested in. Nervertheless it is interesting to compare the binary images obtained with thresholding techniques for the two classes (1 phase) problem in order to assess the performance of our algorithms when the full classification problem is considered. To cope with the difficulties above mentioned we consider two different approaches based on density mixture estimations (see (Mignotte et al., 2001)) and a variational model formulated in a level set framework (Chan and Vese, 2001).

The proposed algorithms are described in the next sections. The results obtained with classical (global and local thresholding or the popular k-means algorithm) techniques for the 2 classes (1 phase) problem are also reported for comparison. In particular we used the original Otsu's method (Otsu, 1979) and the Ridler-Calvard technique (Ridler and Calvard, 1978). We show the results obtained in figures 3 and 4 (d) and e)).

2.1 Density Mixture Estimation

In the case of the density mixture estimations framework the original magnitude images have been preprocessed in order to eliminate the high frequencies associated to noise and to increase the low contrast present in some parts of the image. As in (Brinkmann and Manduca, 1998), (Pérez et al., 2004). We consider a low pass homomorphic filter in the frequency domain which has been successfully used in previous works.

The initial pre-processing step is performed with a homomorphic filter in order to correct the gray scale inhomogeneity field. These inhomogeneities are known to appear in MR images as systematic changes in the local statistical characteristics of tissues and are often quite subtle to the human eye. However, even inhomogeneities that are invisible to the human observer alter tissue characteristics enough to hamper automated and semi-automated classification.

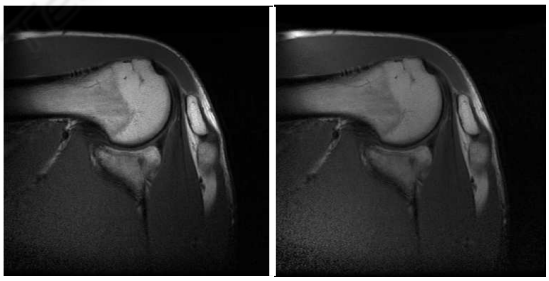

Figure 2: On the left the original image and on the right the pre-processed, corrected image.

Then, in a denoising step, the homogenized image is then filtered again with an adaptative filter to produce 2D wiener denoised sequence of the original image. The denoised slices are then normalized using a dynamical range operator in order to increase the (low) contrast present in the images. We then characterized the different soft tissues and bony structures in 4 classes (bone, muscle, cartilage, fat) partitioning the shoulder complex estimating their initial parameter statistics.

In order to show the basic steps of the algorithm we follow the Bayesian mixture parameter estimation method proposed by (Mignotte et al., 2001)

Let $Z = (X,Y)$ define two random fields where $Y = \{Y_s, s \in S\}$ represents the field of observations corresponding to the pixels of the MR image and $X = \{X_s, s \in S\}$ corresponds to the label field representing the segmented image. Following a Bayesian approach, the posterior distribution of (X,Y), $P(x|y)$, will result by combining the prior distribution, assumed to be stationary and Markovian,

$$P(x) = exp\{-\sum_{<s,t>} \beta(1-\delta(x_s,x_t))\},$$

and the site-wise likelihood $P(y_s|x_s)$, modelled as a mixture of densities

$$P(y_s|x_s,k,\Phi_k) = \sum_{k=1}^{K} \pi_k P(y_s|x_s,k,\Phi_k)$$

where π_k are the mixing proportion ($\sum_k \pi_k = 1$) and where $P(y_s|x_s,k,\Phi_k)$ define Gaussian distributions, with parameters $\Phi_k = (\mu_k, \sigma_k^2)$ in each segmented class k.

Let $\Phi = (\Phi_1, \Phi_2, \ldots, \Phi_K)$ and $\pi = (\pi_1, \pi_2, \ldots, \pi_K)$. In order to proceed with the segmentation procedure, we perform the following algorithm:

0. Initialize parameters $(\Phi^{[0]}, \pi^{[0]})$.

Given $(\Phi^{[p]}, \pi^{[p]})$, we can calculate $(\Phi^{[p+1]}, \pi^{[p+1]})$ by

1. Using the Gibbs sampler, simulate one realization x from the posterior distribution $P(x|y)$ with parameter $(\Phi^{[p]}, \pi^{[p]})$.
2. Define $(\Phi^{[p+1]}, \pi^{[p+1]})$ as the ML estimation of the data (Y,x)
3. Repeat till convergence is achieved.

2.2 Active Contours Without Edges

Since the work of Kass (Kass et al., 1987) is well known that the segmentation problem of digital images can be dealt with in the framework of variational calculus. Nevertheless in medical images there are often no sharp-gradient induced edges at all and region-based active contours driven by gradients can fail in automatic approaches. Recently a new model has been suggested by Chan-Vese which can be deduced from the Mumford -Shah minimal partition problem, (Mumford and Shah, 1989), a basic problem in computer vision. Successful applications of this method have been reported in many papers and fields (see (Chan and Vese, 2001) and (Vese and Chan, 2002)). Our aim is to show that this active contour without edges model (or statistical feature driven model) can be used to solve the classification problem we consider here where a multiphase level set framework for image segmentation is implemented. The basic idea is that, fixed the number of classes in which we are interested in (fat, bone regions, muscle and tendons, ligaments and cartilage), it is sufficient to consider a two phase model, say ϕ_1, ϕ_2, in order to provided partition of the image in four classes (($\phi_1 > 0$ and $\phi_2 > 0$), ($\phi_1 < 0$ and $\phi_2 > 0$), ($\phi_1 > 0$ and $\phi_2 < 0$), ($\phi_1 < 0$ and $\phi_2 < 0$)).

Now, we explain the one phase (binary) and two phases models considered in the experiments. Let $\Omega \subset I\!R^2$ be an open, bounded domain (usually a square) where $(x,y) \in \Omega$ denotes pixel location and $I(x,y)$ is a function representing the intensity image values. Let moreover the level sets functions denoted by $\phi_1, \phi_2 : \Omega \to I\!R$. The union of the zero-level sets of ϕ_1 and ϕ_2 represents the edges of segmentation. Using this formalism the functions ϕ_1 and ϕ_2 can be characterized as the minimum of the following energy functional:

$$\begin{aligned} F(C,\Phi) &= \int_\Omega (I-c_{11})^2 H(\phi_1)H(\phi_2)dxdy \\ &+ \int_\Omega (I-c_{10})^2 H(\phi_1)(1-H(\phi_2))dxdy \\ &+ \int_\Omega (I-c_{01})^2 (1-H(\phi_1))H(\phi_2)dxdy \\ &+ \int_\Omega (I-c_{00})^2 (1-H(\phi_1))(1-H(\phi_2))dxdy \\ &+ \nu \int_\Omega |\nabla H(\phi_1)|dxdy + \\ &+ \nu \int_\Omega |\nabla H(\phi_2)|dxdy \end{aligned} \quad (1)$$

where $C = (c_{11}, c_{10}, c_{01}, c_{00})$ is a constant vector representing the mean of each region (or class), $\Phi = (\phi_1, \phi_2)$, ν is a parameter of smoothness and $H(x)$ is the Heaviside function, $H(x) = 1$ if $x \geq 0$ and $H(x) = 0$ otherwise,

The Euler-Lagrange equations obtained by minimizing (1) with respect to C and Φ are solved with a gradient descent method leading to the coupled parabolic PDE system (Vese and Chan, 2002):

$$\begin{aligned} \frac{\partial \phi_1}{\partial t} &= \delta_\varepsilon(\phi_1)\left\{\nu\nabla\cdot\left(\frac{\nabla\phi_1}{|\nabla\phi_1|}\right) - \right. \\ &- \left[(I-c_{11})^2 - (I-c_{01}^2)\right]H(\phi_2) + \\ &+ \left.\left[(I-c_{10})^2 - (I-c_{00}^2)\right](1-H(\phi_2))\right\} \end{aligned} \quad (2)$$

$$\begin{aligned} \frac{\partial \phi_2}{\partial t} &= \delta_\varepsilon(\phi_2)\left\{\nu\nabla\cdot\left(\frac{\nabla\phi_2}{|\nabla\phi_2|}\right) - \right. \\ &- \left[(I-c_{11})^2 - (I-c_{01}^2)\right]H(\phi_1) + \\ &+ \left.\left[(I-c_{10})^2 - (I-c_{00}^2)\right](1-H(\phi_1))\right\}. \end{aligned} \quad (3)$$

Where δ_ε denotes a smooth (not compactly supported) approximation to the Dirac delta distribution. Notice that the equations (2) and (3) are (weakly) coupled in the lower order terms. In case of two regions only one level set function ϕ is needed. The resulting one phase energy functional to minimize is as follows:

$$\begin{aligned} E_{cv}(c_1,c_0,\phi) &= \nu\int_\Omega |\nabla H(\phi)|dxdy + \\ &+ \int_\Omega H(\phi)|I(x,y)-c_1|^2dxdy + \\ &+ \int_\Omega (1-H(\phi))|I(x,y)-c_0|^2dxdy \end{aligned} \quad (4)$$

and the associated gradient descent equation is :

$$\begin{aligned} \frac{\partial\phi}{\partial t} &= \delta_\varepsilon(\phi)\left[\nu\nabla\cdot\left(\frac{\nabla\phi}{|\nabla\phi|}\right) - \right. \\ &- \left. |I(x,y)-c_1|^2+|I(x,y)-c_0|^2\right]. \end{aligned} \quad (5)$$

The equations (2), (3) or (5) have to be complemented with feasible (due to the non-uniqueness of the corresponding steady states) initial conditions and homogeneous boundary conditions of Neumann type (no flux). As in Chan and Vese (Chan and Vese, 2001) the steady states associated to system (2), (3) or the eq. (5) can be asymptotically reached by using a gradient descent method where δ_ε is substituted by 1 (this is possible because δ_ε has no compact support). Numerically, as we are concerned with the quality of the classification and not in to speed it up, we used a simple first order (in time) Euler explicit finite difference scheme and weighted, centered, second order formulas in space, with a regularization of the (degenerate) diffusion term to avoid division by zero (which occurs in homogeneous, very low gradient regions which are located far from the active contour and do not affect the final segmentation as soon as the regularizing parameter is small). The time steps have been choosen accordingly in order to preserv numerical stability and convergence.

3 RESULTS

We present the results obtained by applying the above methods to a pair of slices extracted from a volume MRI sequence of the shoulder complex. The slices dimensions are 512x512.

Binary segmentations obtained with both methods (the bayesian density mixture estimation and the PDE-based hybrid active contours method without edges) are shown in Figures 3-4 before of the multiphase classification, see figures 5-6.

Figure 3: Slice 1. Segmentation image for one phase (2 classes) with: a) k-means b) Density mixture c) Active contours without edges d) Otsu's and e) Ridler Calvard algorithms.

For comparison and in both cases, we also include the results provided by classical methods. Binary segmentation is also used to assess the parameters involved in the model equations and to provide automatic, robust initial conditions for the evolutive problem in the multiphase case.

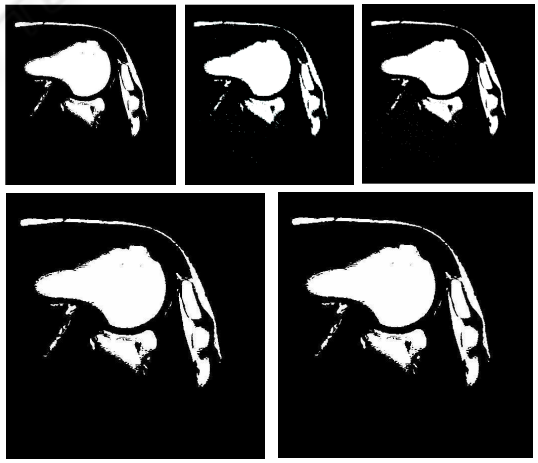

Figure 4: Slice 2. Segmentation image for one phase (2 classes) with: a) k-means b) Density mixture c) Active contours without edges d) Otsu's and e) Ridler Calvard algorithms.

In Figures 3-4 we see that in both cases the bony structures (head of scapula, head of humerus, clavicle, acromion) are properly classified. Background, skin, and muscle are also characterized in the binary images as the soft (tissue) class. Visual inspection

suggests convergence to the same limit solution. This is indeed confirmed when the differences images are computed and classical methods (first row) are compared.

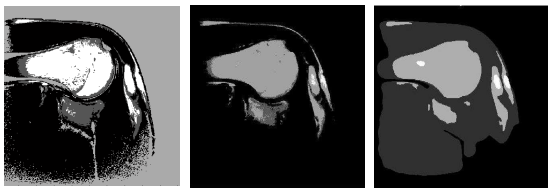

Figure 5: Slice 1. Segmentation image for two phases (4 classes) a) k-means b) Density mixture c) Active contours without edges algorithms.

As aspected, some more differences between the quality reconstruction of the different methods can be appreciated in the multiphase (four classes) classification problem. In Figures 5-6 we report the results obtained with the classical (k-means) algorithm (left), the bayesian mixture model (center) and the Chan-Vese model (right). The greater tubercle and the head of the humerus are properly classified and shaped with our methods (center and right) while the classical k-means fails in both aspects (and in both slices, see Figures 5-6, on the left, where the bone is under-estimated and muscle is wrongly detected). Articular cartilage has been detected in (center and right) but not in (left). Muscle is properly classified with the Chan-Vese model (right) and the classical method (left) but no classification has been done in the bayesian approach where the background is assigned to the same class. At the same time the head of the scapula has been properly classified in (right) but not in (center) where the shape, nevertheless is correctly obtained. Notice also that the acromial process has been characterized by the two methods.

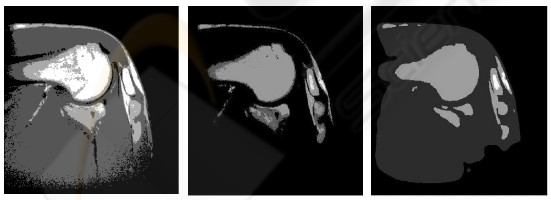

Figure 6: Slice 2. Segmentation image for two phases (4 classes) a) k-means b) Density mixture c) Active contours without edges algorithms.

4 CONCLUSIONS

We considered the problem of automatic segmentation of 2D images using an hybrid, statistical and geometrical model based on Chan-Vese work. This method provides correct classification of bony structures but soft tissues are not yet properly classified. This is also manifested in the bayesian approach. The differences between the results obtained with the two methods suggest the conclusion that hybrid methods can give better results as far as the right statistics are included in the model and this will be the aim of our future work.

ACKNOWLEDGEMENTS

This work was partially granted by ”Research on Molecular and Multimodality Medical Imaging Network” of the Carlos III Health Institute. Finally the authors of the present work would like to thank Ruber International Hospital and the neuroradiologist Dr. Juan Linera.

REFERENCES

Biviji, A., Paiement, G., Davidsion, A., and Steinbach, L. (2002). Musculoeskeletal manifestations of the human immunodeficiency virus infection. *Of the American Academy of Orthopedic Surgeons*, pages 10:312–20.

Brinkmann, B. and Manduca, A. (1998). Optimized homomorphic unsharp masking for mr grayscale inhomogeneity correction. In *IEEE transactions on medical imaging, p. 62-66*, volume 17.

Chan, T. F. and Vese, L. A. (2001). Active contours without edges. ieee transactions on image processing. In *IEEE Transactions on Image Processing*, volume 10.

Ehman, R., Megibow, A., MacCauley, T., Bluemke, D., and Steinbach, L. (2001). Musculoskeletal imaging. In *the 24th Annual Course of the Society of Computed Body Tomography and Magnetic Resonance*, Miami.

Johnson, R. and Steinbach LS, e. (2003). Essentials of musculoskeletal imaging. american academy of orthopedic surgeons. Chicago.

Kass, M., WitKin, A., and Terzopoulos, D. (1987.). Snakes: Active contour models. In *Intl. J. Comput. Vision, 1:321-331*.

Mignotte, M., Meunier, J., Soucy, J. P., and Janicki, C. (2001). classification of brain spect images using 3d markov random field and density mixture estimations. 5th world multi-conference on systemics, cybernetics and informatics. In *Concepts and Applications of Systemics and Informatics*, volume 10, pages 239–244, Orlando.

Mumford, D. and Shah, J. (1989). Optimal approximation by piecewise smooth functions and associated variational problems. In *Communications on Pure Applied Mathematics, p. 577-685*, volume 42.

Otsu, N. (1979). A threshold selection method from gray level histograms. *IEEE transactions on systems, man, and cybernetics*, 9(1):62–66.

Pérez, G., Diez, R. M., Hernández, J. A., and José San Martín (2004). A new approach to automatic segmentation of bone in medical magnetic resonance imaging. In *5th International Symposium, ISBMDA*, pages 21–26, Spain.

Ridler, T. and Calvard, S. (1978). Picture thresholding using an iterative selection method. *IEEE transactions on systems, man, and cybernetics*, 8(8).

Vahlensieck, M. (2000). Mri of the shoulder. *European Radiology*, 10(2):242–249.

Vese, L. A. and Chan, T. F. (2002). A multiphase level set framework for image segmentation using the mumford and shah model. In *International Journal of Computer Vision, p. 271-293*, volume 50.